Advances in Nuclear Many-Body Theory
June 7 - 10, 2011, Primošten, Croatia

Covariant density functional theory for magnetic rotation

Pengwei Zhao(赵鹏巍)

Supervisor： Prof. Jie Meng (孟杰)

School of Physics, Peking University

Collaborators: Haozhao Liang, Jing Peng, Peter Ring, and Shuangquan Zhang

Outline

Rotation bands in nuclei

- Substantial quadrupole deformation
- Strong electric quadrupole (E2) transitions
- Coherent collective rotation of many nucleons around an axis perpendicular to the symmetry axis.

  Bohr and Mottelson, *"Nuclear Structure"*, 1975

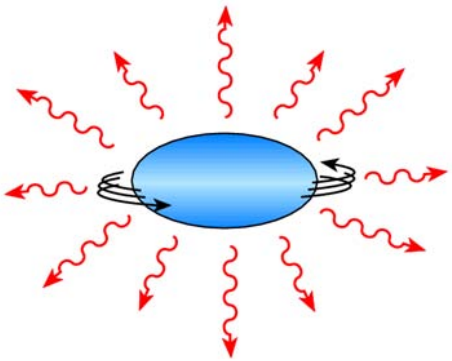

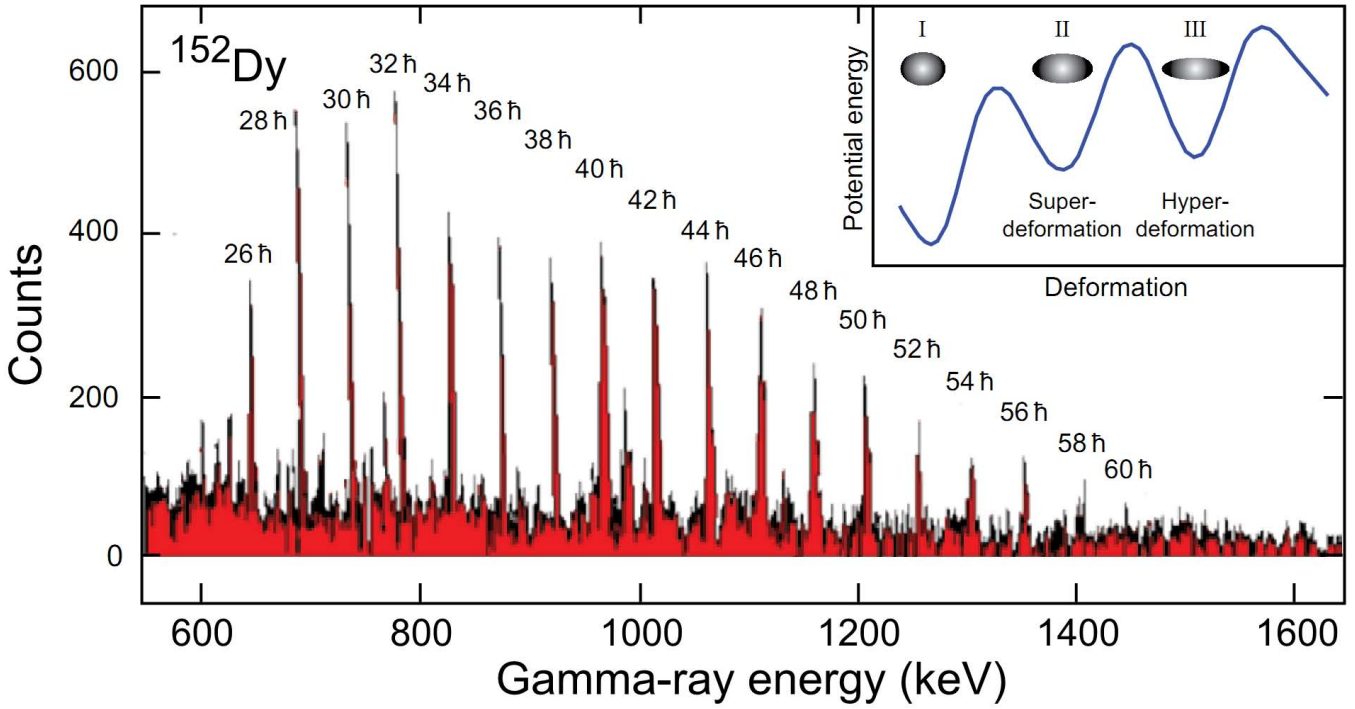

Rotation bands in nuclei

- Long cascades of magnetic dipole (M1) transitions in neutron deficient Pb nuclei

  Clark et al., PLB1992; Baldsiefen et al., PLB1992; Kuhnert et al., PRC1992

  ⋆ Near spherical or weakly deformed nuclei

  ⋆ Strong M1 transitions

  ⋆ Very weak E2 transtions

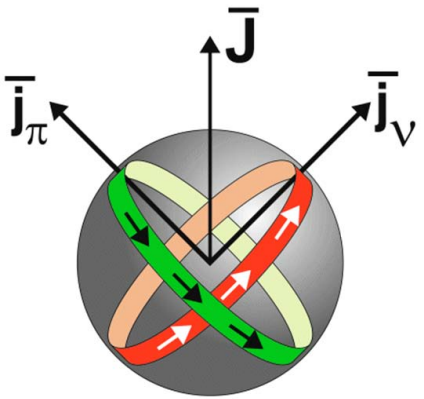

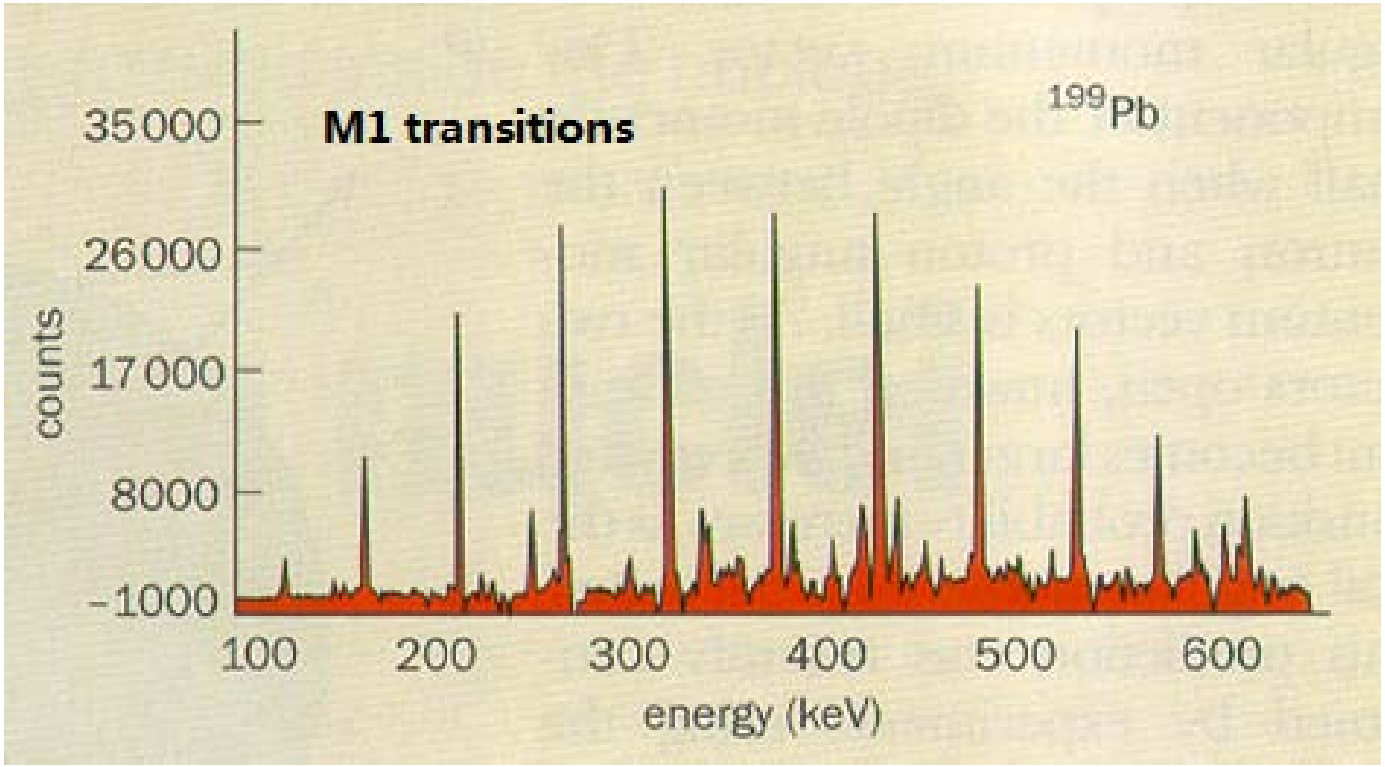

Magnetic rotation

- Magnetic rotation Frauendorf, Meng, Reif, 1994
  a. near spherical or weakly deformed nuclei
  b. rotational bands with $\Delta I = 1$
  c. strong M1 transitions and very weak E2 transitions
  d. shears mechanism

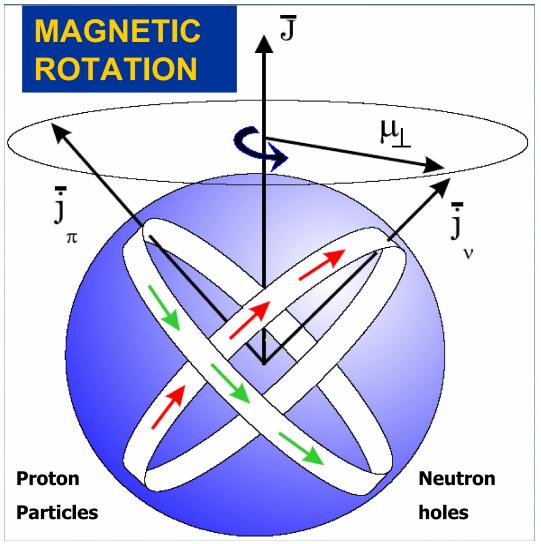

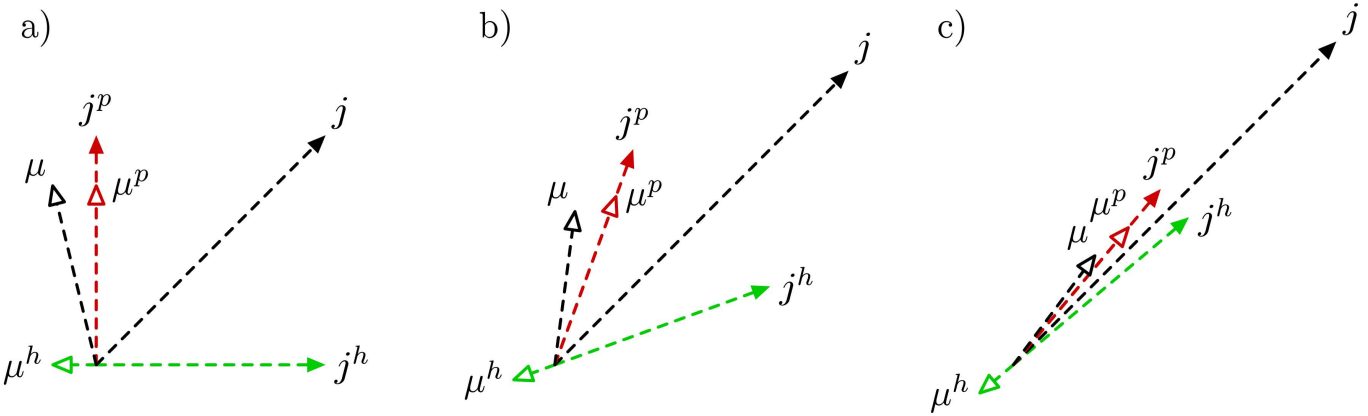

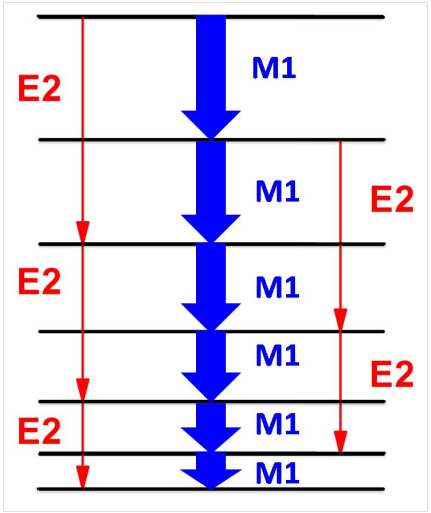

Magnetic rotation bands

- Experimentally
  a. long cascades of M1 transitions in the neutron deficient Pb nuclei
     Clark et al., PLB1992; Baldsiefen et al., PLB1992; Kuhnert et al., PRC1992
  b. clear evidence: lifetime measurements for four M1-bands in $^{198,199}\mathrm{Pb}$
     Clark et al., PRL1997
  c. in $A \sim 80$, $A \sim 110$ and $A \sim 140$ regions
     Amita et al., ADNDT2000
  d. $^{60}\mathrm{Ni}$: the lightest system in which magnetic rotation has been observed up to date
     Torres et al., PRC2008

- Tilted Axis Cranking (TAC) model (Beyond 1D-Cranking)
  a. the first fully self-consistent TAC solutions base on Nilsson model .
     Frauendorf, NPA1993
  b. qualities of the TAC approximation have been tested with the particle rotor model.
     Frauendorf and Meng, ZPA1996
  c. semi-phenomenological models: pairing-plus-quadrupole-quadrupole TAC (PQTAC).
     Frauendorf, NPA2000
  d. fully microscopic investigations: (covariant) density functional theory
     Madokoro et al., PRC2000, Olbratowski et al., PRL2004

Covariant density functional theory – Cranking version

Covariant density functional theory (CDFT) has achieved great success in describing lots of nuclear phenomena in stable as well as exotic nuclei.

Covariant density functional theory – Cranking version

Covariant density functional theory (CDFT) has achieved great success in describing lots of nuclear phenomena in stable as well as exotic nuclei.

- Cranking model based on CDFT (Cranking Relativistic Mean-Field (RMF))
  a. without any additional parameters in describing rotational excitations.
  b. 3D-Cranking RMF: Magnetic rotation in $^{84}\mathrm{Rb}$.
  Madokoro, Meng, Matsuzaki, Yamaji, PRC 62, 061301 (2000)
  c. 2D-Cranking RMF: Systematic investigations of magnetic rotation.
  Peng, Meng, Ring, Zhang, PRC 78, 024313 (2008)

- RMF model based on the point-coupling (PC) interaction
  Nikolaus et al., PRC1992; Bürvenich et al., PRC2002; PWZ, Li, Yao, Meng, PRC2010
  a. avoid the possible physical constrains introduced by explicit usage of the Klein-Gordon equation to describe mean meson fields, especially the fictitious σ meson.
  b. possible to study the role of naturalness in effective theories for nuclear structure related problem.
  c. provide more opportunity to investigate its relationship to the nonrelativistic approaches.

Covariant density functional theory – Cranking version

Covariant density functional theory (CDFT) has achieved great success in describing lots of nuclear phenomena in stable as well as exotic nuclei.

- Cranking model based on CDFT (Cranking Relativistic Mean-Field (RMF))
  a. without any additional parameters in describing rotational excitations.
  b. 3D-Cranking RMF: Magnetic rotation in ^{84}Rb.
  Madokoro, Meng, Matsuzaki, Yamaji, PRC 62, 061301 (2000)
  c. 2D-Cranking RMF: Systematic investigations of magnetic rotation.
  Peng, Meng, Ring, Zhang, PRC 78, 024313 (2008)

- RMF model based on the point-coupling (PC) interaction
  Nikolaus et al., PRC1992; Bürvenich et al., PRC2002; PWZ, Li, Yao, Meng, PRC2010
  a. avoid the possible physical constrains introduced by explicit usage of the Klein-Gordon equation to describe mean meson fields, especially the fictitious σ meson.
  b. possible to study the role of naturalness in effective theories for nuclear structure related problem.
  c. provide more opportunity to investigate its relationship to the nonrelativistic approaches.

In the present work: **PWZ, Zhang, Peng, Liang, Ring, Meng, PLB2011**

- The self-consistent TAC-RMF theory with PC interaction is established.
- Investigate the newly observed shears bands in ^{60}Ni systematically as an example.

Tilted axis cranking relativistic point-coupling model

- The Lagrangian is transformed to the frame rotating with the uniform velocity
  Koepf NPA1989; Kaneko PLB1993; Madokoro PRC1997

$$\Omega = (\Omega_x, 0, \Omega_z) = (\Omega\cos\theta_\Omega, 0, \Omega\sin\theta_\Omega) \tag{1}$$

$$x^\alpha = \begin{pmatrix} t \\ \boldsymbol{x} \end{pmatrix} \rightarrow \tilde{x}^\mu = \begin{pmatrix} \tilde{t} \\ \tilde{\boldsymbol{x}} \end{pmatrix} = \begin{pmatrix} 1 & \boldsymbol{0} \\ \boldsymbol{0} & \boldsymbol{R} \end{pmatrix} \begin{pmatrix} t \\ \boldsymbol{x} \end{pmatrix} \tag{2}$$

- Dirac equation:

$$\left[\boldsymbol{\alpha}\cdot(-i\boldsymbol{\nabla} - \boldsymbol{V}(\boldsymbol{r})) + \beta\left(m + S(\boldsymbol{r})\right) + V(\boldsymbol{r}) - \boldsymbol{\Omega}\cdot\hat{\boldsymbol{J}}\right]\psi_\alpha = \epsilon\psi_\alpha \tag{3}$$

  with $\hat{\boldsymbol{J}} = \hat{\boldsymbol{L}} + \frac{1}{2}\hat{\boldsymbol{\Sigma}}$

- Potential:

$$S(\boldsymbol{r}) = \alpha_S\rho_S + \beta_S\rho_S^2 + \gamma_S\rho_S^3 + \delta_S\triangle\rho_S, \tag{4}$$

$$V^\mu(\boldsymbol{r}) = \alpha_V j_V^\mu + \gamma_V(j_V^\mu)^3 + \delta_V\triangle j_V^\mu + \tau_3\alpha_{TV} j_{TV}^\mu + \tau_3\delta_{TV}\triangle j_{TV}^\mu + e\frac{1-\tau_3}{2}A^\mu \tag{5}$$

- Spatial components of vector field are involved due to the time-reversal invariance broken, and the terms $\propto \Omega^2$ are neglected similar to the meson-exchange version.

Observables

- Binding energy:

$$
\begin{aligned}
E_{\rm tot} = & \sum_{k=1}^{A} \epsilon_k - \int d^3r \left\{ \frac{1}{2}\alpha_S \rho_S^2 + \frac{1}{2}\alpha_V j_V^\mu (j_V)_\mu + \frac{1}{2}\alpha_{TV} j_{TV}^\mu (j_{TV})_\mu \right. \\
& + \frac{2}{3}\beta_S \rho_S^3 + \frac{3}{4}\gamma_S \rho_S^4 + \frac{3}{4}\gamma_V (j_V^\mu (j_V)_\mu)^2 + \frac{1}{2}\delta_S \rho_S \triangle \rho_S + \frac{1}{2}\delta_V (j_V)_\mu \triangle j_V^\mu \\
& \left. + \frac{1}{2}\delta_{TV} j_{TV}^\mu \triangle (j_{TV})_\mu + \frac{1}{2} e j_p^0 A_0 \right\} + \sum_{k=1}^{A} \langle k | \boldsymbol{\Omega} \cdot \hat{\boldsymbol{J}} | k \rangle
\end{aligned} \tag{6}
$$

- Total angular momentum

$$
\langle \hat{J} \rangle^2 = I(I+1) \tag{7}
$$

- Quadrupole moments and magnetic moments

$$
Q_{20} = \sqrt{\frac{5}{16\pi}} \langle 3z^2 - r^2 \rangle, \quad Q_{22} = \sqrt{\frac{15}{32\pi}} \langle x^2 - y^2 \rangle \tag{8}
$$

$$
\boldsymbol{\mu} = \sum_i^A \int d^3r \left[\frac{mc^2}{\hbar c} Q_i \psi_i^\dagger(\boldsymbol{r}) \boldsymbol{r} \times \boldsymbol{\alpha} \psi_i(\boldsymbol{r}) + \kappa_i \psi_i^\dagger(\boldsymbol{r}) \beta \boldsymbol{\Sigma} \psi_i(\boldsymbol{r}) \right]. \tag{9}
$$

where $Q_p = 1$, $Q_n = 0$, $\kappa_p = 1.793$, and $\kappa_n = -1.913$.

Observables

- Binding energy:

$$E_{\rm tot} = \sum_{k=1}^{A}\epsilon_k - \int d^3r \left\{\frac{1}{2}\alpha_S\rho_S^2 + \frac{1}{2}\alpha_V j_V^\mu (j_V)_\mu + \frac{1}{2}\alpha_{TV} j_{TV}^\mu (j_{TV})_\mu \right.$$
$$+\frac{2}{3}\beta_S\rho_S^3 + \frac{3}{4}\gamma_S\rho_S^4 + \frac{3}{4}\gamma_V (j_V^\mu (j_V)_\mu)^2 + \frac{1}{2}\delta_S\rho_S\triangle\rho_S + \frac{1}{2}\delta_V (j_V)_\mu \triangle j_V^\mu$$
$$\left. +\frac{1}{2}\delta_{TV} j_{TV}^\mu \triangle (j_{TV})_\mu + \frac{1}{2}e j_p^0 A_0 \right\} + \sum_{k=1}^{A}\langle k|\boldsymbol{\Omega}\cdot\hat{\boldsymbol{J}}|k\rangle \tag{6}$$

- Total angular momentum

$$\langle \hat{J}\rangle^2 = I(I+1) \tag{7}$$

- Quadrupole moments and magnetic moments

- $B(M1)$ and $B(E2)$ transition probabilities

$$B(M1) = \frac{3}{8\pi}\mu_\perp^2 = \frac{3}{8\pi}(\mu_x \sin\theta_J - \mu_z \cos\theta_J)^2 \tag{8}$$

$$B(E2) = \frac{3}{8}\left[Q_{20}\cos^2\theta_J + \sqrt{\frac{2}{3}}Q_{22}(1+\sin^2\theta_J)\right]^2 \tag{9}$$

Numerical details

- Nucleus: $^{60}\mathrm{Ni}$;
- Harmonic oscillator shells: $N_f = 10$;
- Parameter set: PC-PK1; PWZ, Li, Yao, Meng, PRC2010
- Configurations:

M-1	Config1	$\pi[(1f_{7/2})^{-1}(fp)^{1}]$	$\nu[(1g_{9/2})^{1}(fp)^{3}]$
	Config1*	$\pi[(1f_{7/2})^{-1}(fp)^{1}]$	$\nu[(1g_{9/2})^{1}(fp)^{4}(1f_{7/2})^{-1}]$
M-2	Config2	$\pi[(1f_{7/2})^{-1}(1g_{9/2})^{1}]$	$\nu[(1g_{9/2})^{1}(fp)^{3}]$
M-3	Config3	$\pi[(1f_{7/2})^{-1}(fp)^{1}]$	$\nu[(1g_{9/2})^{2}(fp)^{2}]$
	Config3*	$\pi[(1f_{7/2})^{-2}(fp)^{2}]$	$\nu[(1g_{9/2})^{2}(fp)^{3}(1f_{7/2})^{-1}]$

- Config1, Config2, and Config3 were proposed for M-1, M-2, and M-3 respectively by Torres et al. Torres et al., PRC2008

Numerical details

- Nucleus: ^{60}Ni;
- Harmonic oscillator shells: $N_f = 10$;
- Parameter set: PC-PK1; PWZ, Li, Yao, Meng, PRC2010
- Configurations:

M-1	Config1	$\pi[(1f_{7/2})^{-1}(fp)^{1}]$	$\nu[(1g_{9/2})^{1}(fp)^{3}]$
	Config1*	$\pi[(1f_{7/2})^{-1}(fp)^{1}]$	$\nu[(1g_{9/2})^{1}(fp)^{4}(1f_{7/2})^{-1}]$
M-2	Config2	$\pi[(1f_{7/2})^{-1}(1g_{9/2})^{1}]$	$\nu[(1g_{9/2})^{1}(fp)^{3}]$
M-3	Config3	$\pi[(1f_{7/2})^{-1}(fp)^{1}]$	$\nu[(1g_{9/2})^{2}(fp)^{2}]$
	Config3*	$\pi[(1f_{7/2})^{-2}(fp)^{2}]$	$\nu[(1g_{9/2})^{2}(fp)^{3}(1f_{7/2})^{-1}]$

- Config1, Config2, and Config3 were proposed for M-1, M-2, and M-3 respectively by Torres et al. Torres et al., PRC2008
- Config1* and Config3* have to be introduced to describe M-1 and M-3 completely.
- For Config3*, the two proton holes are paired, i.e., one is $j_z = 7/2$, the other is $j_z = -7/2$.

Energy spectra

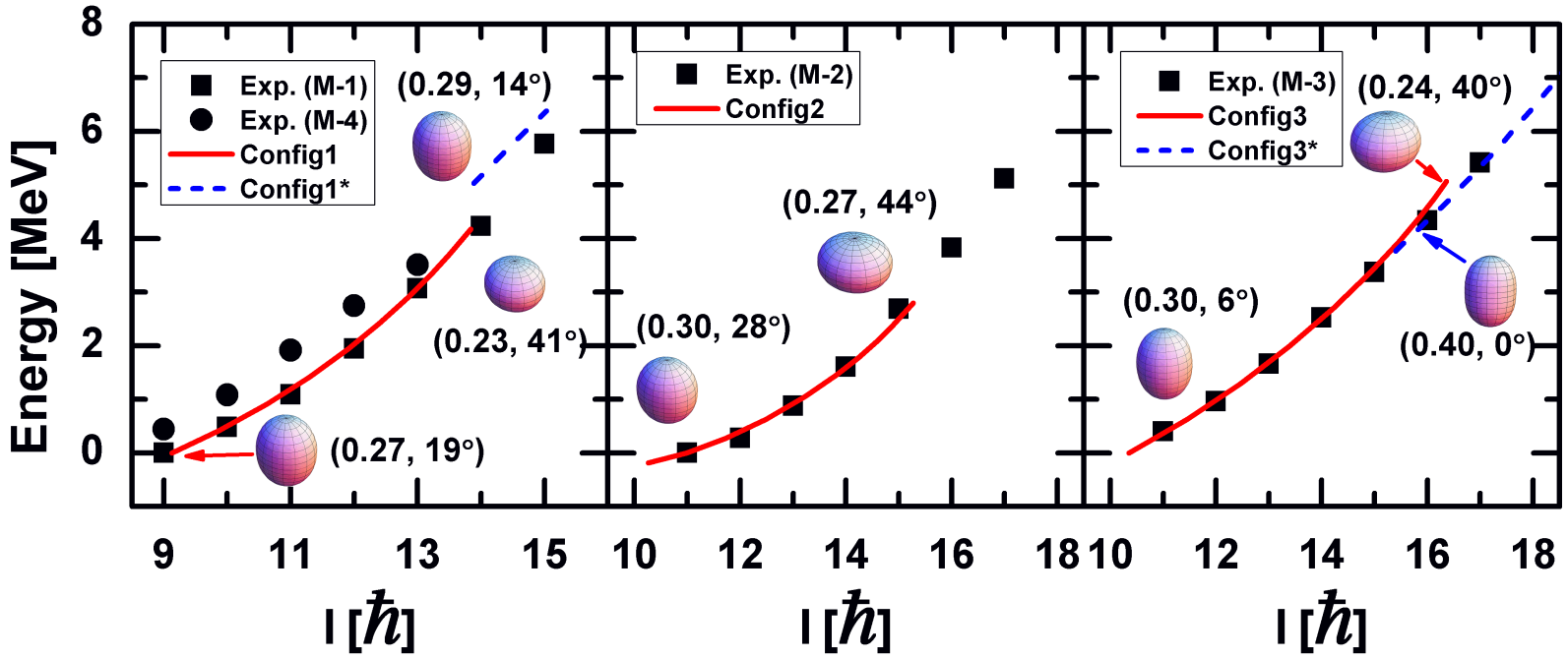

Figure: Energy as a function of the total angular momentum in the tilted axis cranking RMF calculation in comparison with the available data for band M-1 and M-4 (left panel), M-2 (middle panel), as well as M-3 (right panel). The energy at $I = 9\hbar$, $I = 11\hbar$, and $I = 15\hbar$ are taken as references in the left, middle and right panels respectively.

Remarks

a. The experimental energies are reproduced quite well.

b. The appropriate configuration could not be followed up to the largest observed spin.

c. The data for high-spin states in band M-1 and M-3 can be well reproduced with Config1* and Config3*.

Deformation

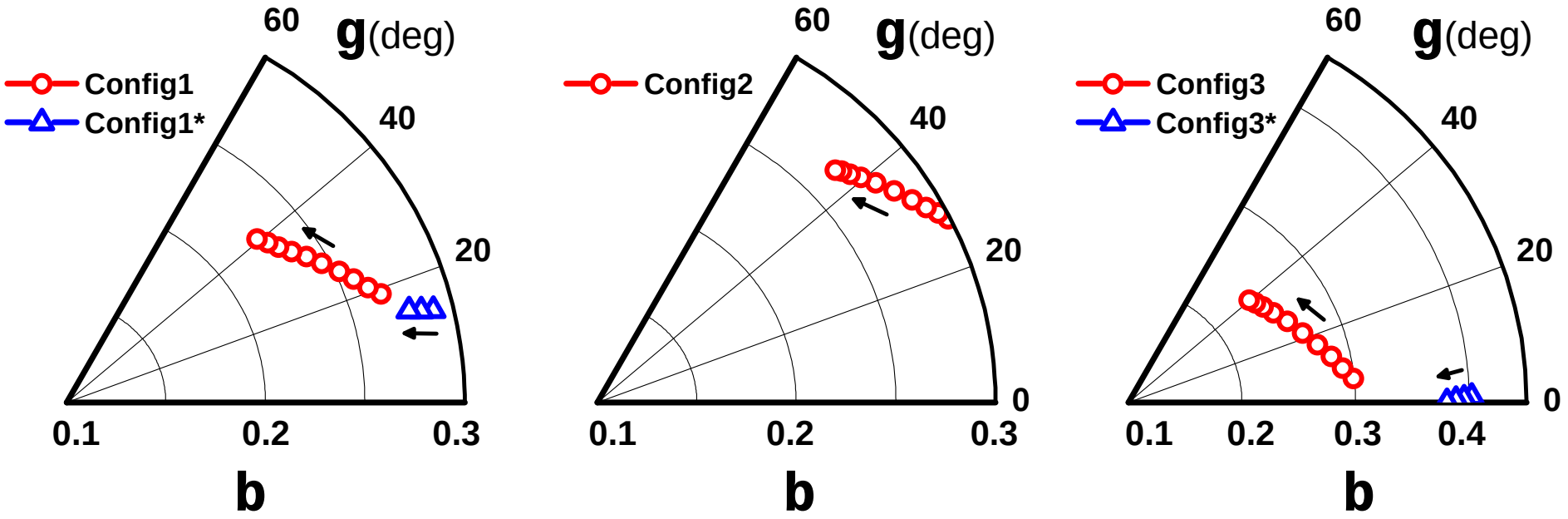

Figure: Deformation parameters as functions of the rotational frequency in the tilted axis cranking RMF calculations.

Remarks

a. β: smoothly decrease; γ: smoothly increase.

b. Config3*: γ reduces to nearly zero.

Angular momentum

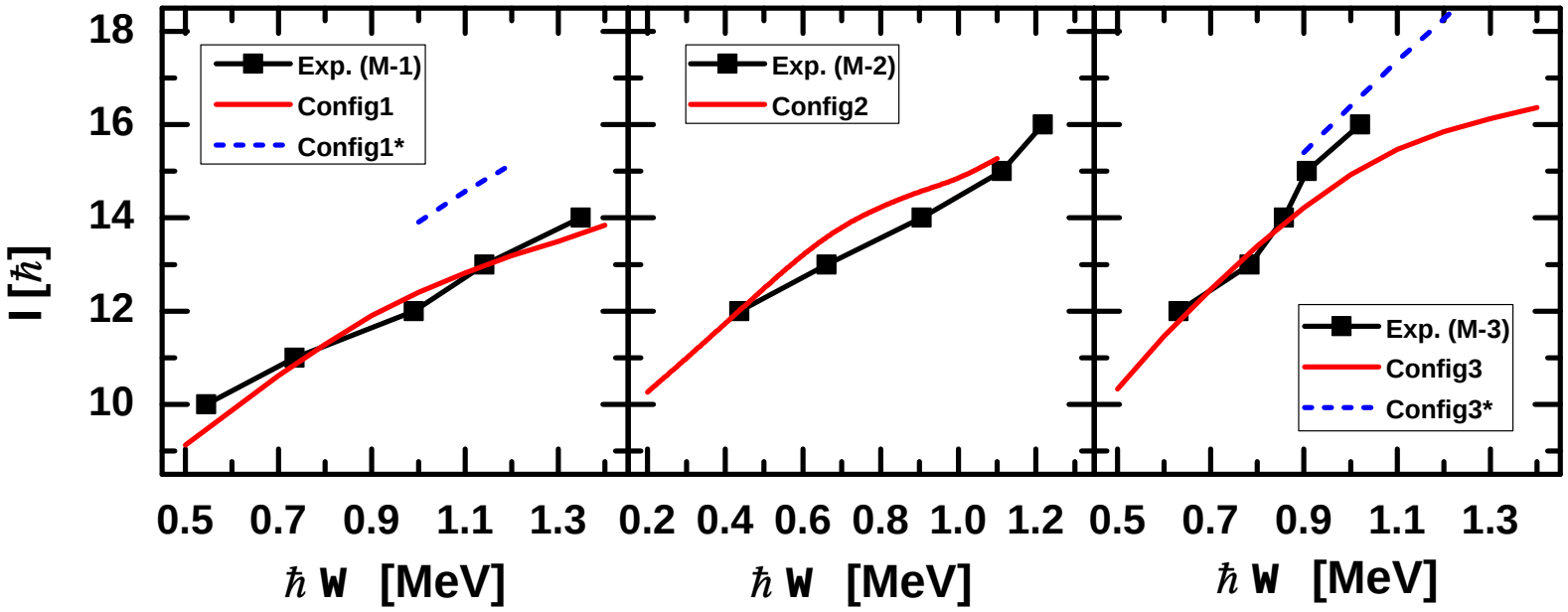

Figure: Total angular momentum as a function of the rotational frequency in tilted axis cranking RMF calculation in comparison with the data for band M-1 (left panel), M-2 (middle panel), as well as M-3 (right panel).

Remarks

a. The calculated total angular momenta well agree with the data which also demonstrates that the relativistic TAC calculations can reproduce the moments of inertial quite well.

b. Observed backbending in M-2 and M-3 bands $\Longrightarrow$ transitions from one configuration to another.

Direction of the total angular momentum vector

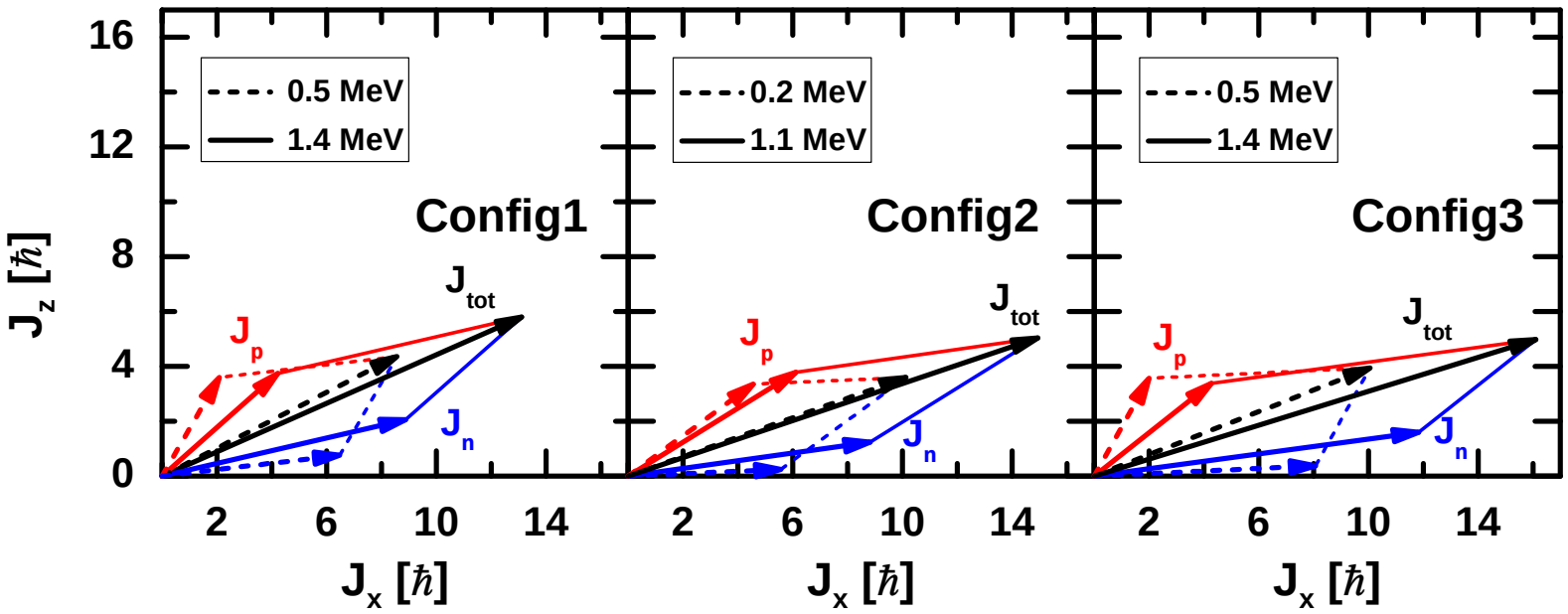

Figure: Composition of the total angular momentum at both the bandhead and the maximum rotational frequency in tilted axis cranking RMF calculations with the configuration of Config1 (left panel), Config2 (middle panel), and Config3 (right panel).

Config1	$\pi[(1f_{7/2})^{-1}(fp)^{1}]$	$\nu[(1g_{9/2})^{1}(fp)^{3}]$
Config2	$\pi[(1f_{7/2})^{-1}(1g_{9/2})^{1}]$	$\nu[(1g_{9/2})^{1}(fp)^{3}]$
Config3	$\pi[(1f_{7/2})^{-1}(fp)^{1}]$	$\nu[(1g_{9/2})^{2}(fp)^{2}]$
Config3*	$\pi[(1f_{7/2})^{-2}(fp)^{2}]$	$\nu[(1g_{9/2})^{2}(fp)^{3}(1f_{7/2})^{-1}]$

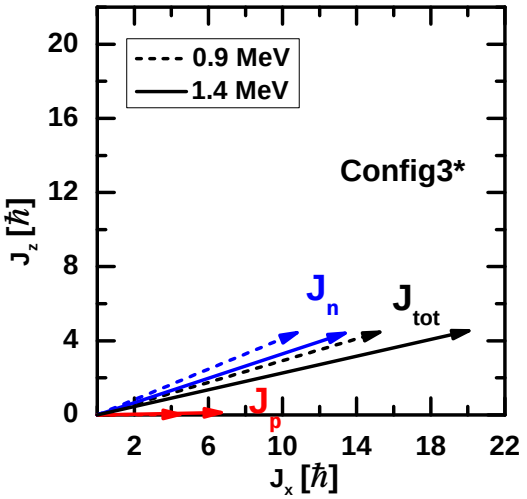

Electromagnetic transition properties

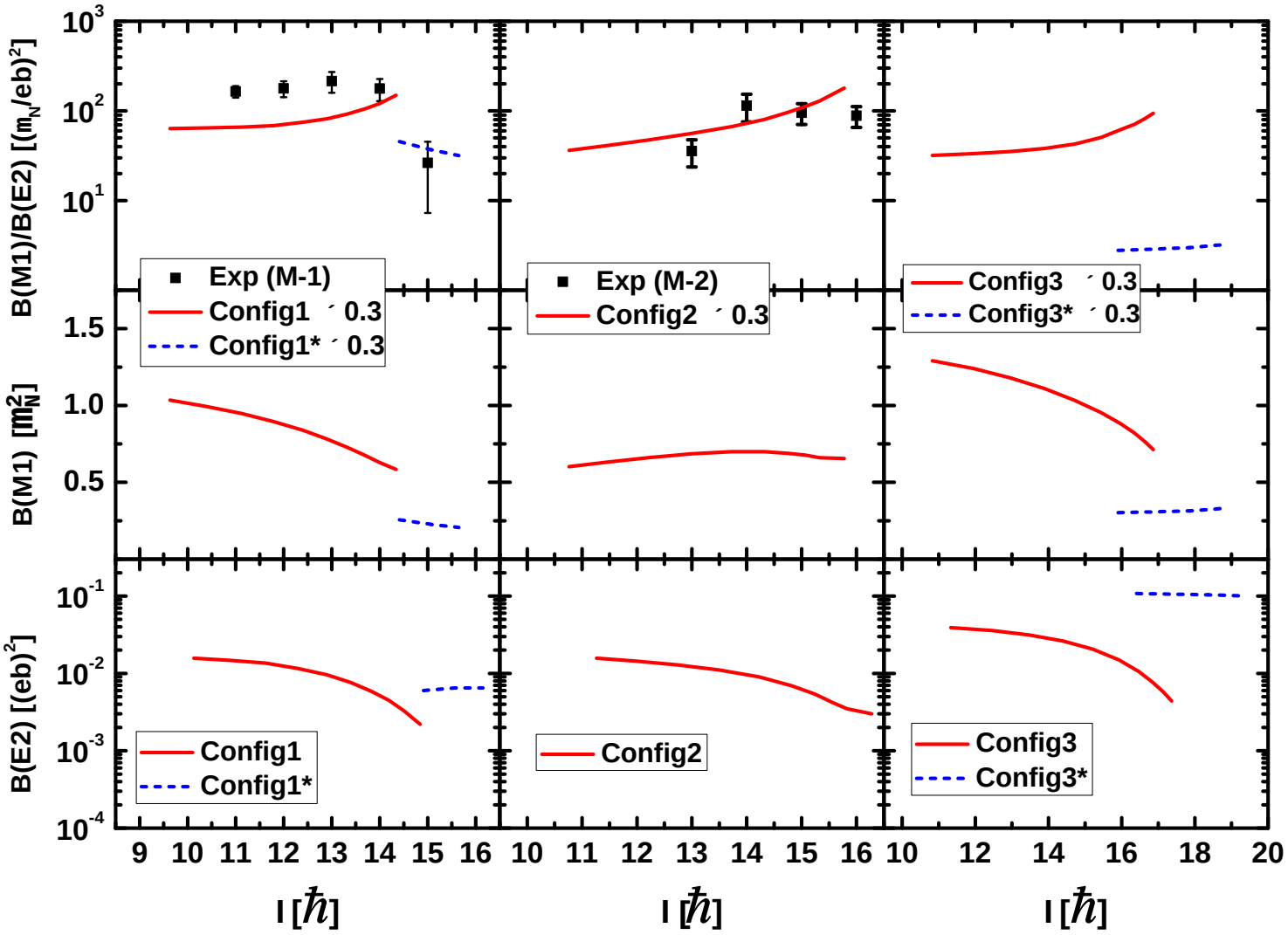

a. The tendency of B(M1)/B(E2) is well reproduced.

b. M-1(M-3): smooth decrease B(M1) $\Longrightarrow$ shears effect.

c. M-2: small decline of shears angles $\Longrightarrow$ near-constant B(M1)

d. The B(E2) values are very small ($< 0.02(eb)^2$

e. Sharp decrease of B(E2 values $\Longrightarrow$ band termination.

f. Attenuating B(M1) values by factor 0.3, the data are reproduced reasonably.

g. Pairing may reduce the B(M1) value.

Summary

- The self-consistent TAC-RMF theory with PC interaction has been established.
- Applied to investigate the newly observed shears bands in $^{60}\mathrm{Ni}$ systematically.
  - ✓ The competition between configurations and transitions from magnetic to electric rotations have to be considered to reproduce the energy spectra as well as the band crossing phenomena.
  - ✓ The tendency of $B(M1)/B(E2)$ is in a good agreement with the data, in particular, the B(M1) values decrease with increasing spin as expected for the shears mechanism.

Summary

- The self-consistent TAC-RMF theory with PC interaction has been established.
- Applied to investigate the newly observed shears bands in ^{60}Ni systematically.
  - ✓ The competition between configurations and transitions from magnetic to electric rotations have to be considered to reproduce the energy spectra as well as the band crossing phenomena.
  - ✓ The tendency of $B(M1)/B(E2)$ is in a good agreement with the data, in particular, the B(M1) values decrease with increasing spin as expected for the shears mechanism.

Thank you!

Relativistic point-coupling model

- Lagrangian density:

$$\mathcal{L} = \mathcal{L}^{\text{free}} + \mathcal{L}^{\text{4f}} + \mathcal{L}^{\text{hot}} + \mathcal{L}^{\text{der}} + \mathcal{L}^{\text{em}}$$

Nikolaus PRC1992; Bürvenich PRC2002

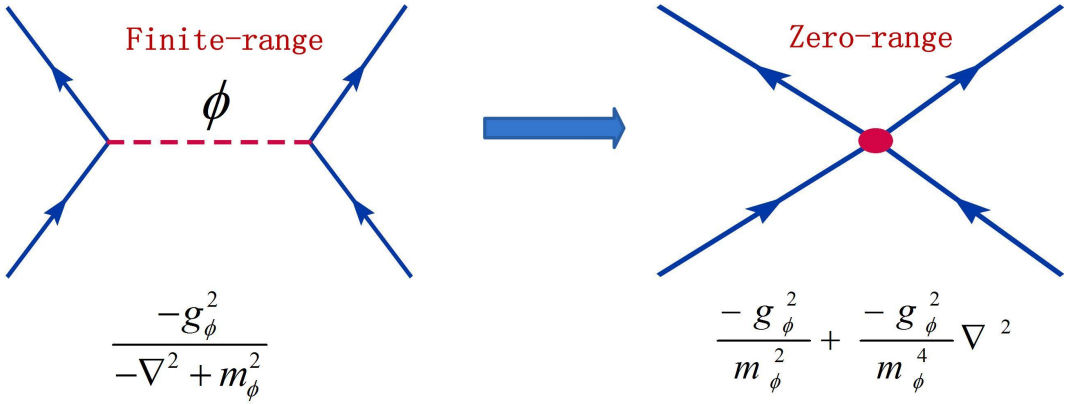

where: 11 effective parameters

$$\mathcal{L}^{\text{free}} = \bar{\psi}(i\gamma_\mu\partial^\mu - m)\psi \tag{10}$$

$$\mathcal{L}^{\text{4f}} = -\frac{1}{2}\alpha_S(\bar{\psi}\psi)(\bar{\psi}\psi) - \frac{1}{2}\alpha_V(\bar{\psi}\gamma_\mu\psi)(\bar{\psi}\gamma^\mu\psi) \tag{11}$$

$$-\frac{1}{2}\alpha_{TS}(\bar{\psi}\vec{\tau}\psi)(\bar{\psi}\vec{\tau}\psi) - \frac{1}{2}\alpha_{TV}(\bar{\psi}\vec{\tau}\gamma_\mu\psi)(\bar{\psi}\vec{\tau}\gamma^\mu\psi) \tag{12}$$

$$\mathcal{L}^{\text{hot}} = -\frac{1}{3}\beta_S(\bar{\psi}\psi)^3 - \frac{1}{4}\gamma_S(\bar{\psi}\psi)^4 - \frac{1}{4}\gamma_V[(\bar{\psi}\gamma_\mu\psi)(\bar{\psi}\gamma^\mu\psi)]^2 \tag{13}$$

$$\mathcal{L}^{\text{der}} = -\frac{1}{2}\delta_S\partial_\nu(\bar{\psi}\psi)\partial^\nu(\bar{\psi}\psi) - \frac{1}{2}\delta_V\partial_\nu(\bar{\psi}\gamma_\mu\psi)\partial^\nu(\bar{\psi}\gamma^\mu\psi)$$

$$-\frac{1}{2}\delta_{TS}\partial_\nu(\bar{\psi}\vec{\tau}\psi)\partial^\nu(\bar{\psi}\vec{\tau}\psi) - \frac{1}{2}\delta_{TV}\partial_\nu(\bar{\psi}\vec{\tau}\gamma_\mu\psi)\partial^\nu(\bar{\psi}\vec{\tau}\gamma_\mu\psi) \tag{14}$$

$$\mathcal{L}^{\text{em}} = -e\frac{1-\tau_3}{2}\bar{\psi}\gamma^\mu\psi A_\mu - \frac{1}{4}F^{\mu\nu}F_{\mu\nu} \tag{15}$$

Relativistic point-coupling model

- Lagrangian density:

$$\mathcal{L} = \mathcal{L}^{\text{free}} + \mathcal{L}^{\text{4f}} + \mathcal{L}^{\text{hot}} + \mathcal{L}^{\text{der}} + \mathcal{L}^{\text{em}}$$

Nikolaus PRC1992; Bürvenich PRC2002

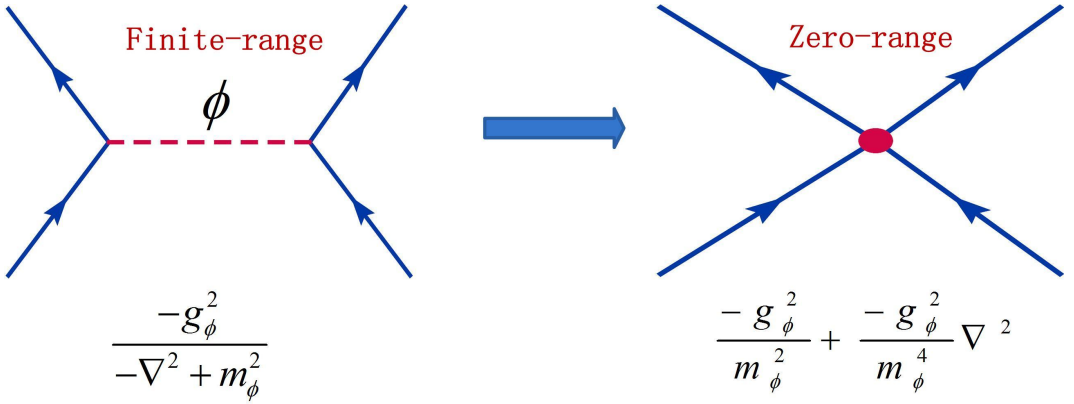

- Mean-field approximation:

$$|\phi\rangle = \prod_{k=1}^{A} a_k^\dagger |0\rangle$$

Relativistic point-coupling model

- Lagrangian density:

$$\mathcal{L} = \mathcal{L}^{\text{free}} + \mathcal{L}^{\text{4f}} + \mathcal{L}^{\text{hot}} + \mathcal{L}^{\text{der}} + \mathcal{L}^{\text{em}}$$

Nikolaus PRC1992; Bürvenich PRC2002

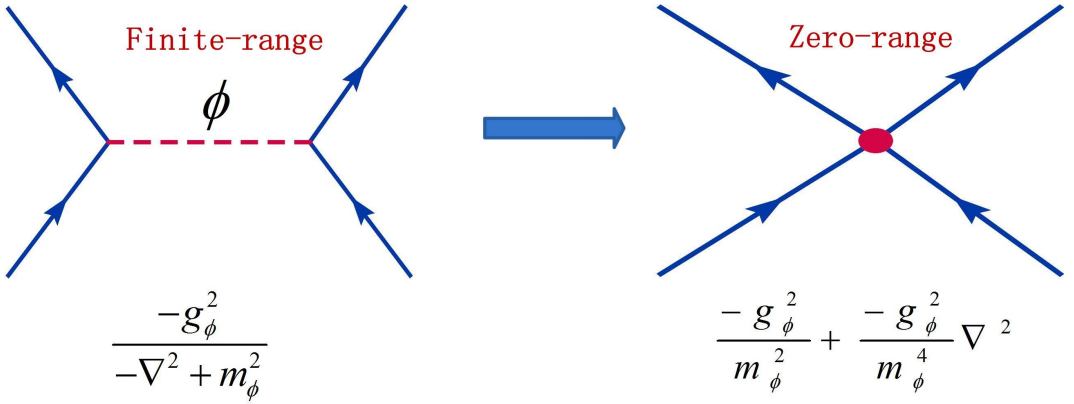

- Mean-field approximation:

$$|\phi\rangle = \prod_{k=1}^{A} a_k^\dagger |0\rangle$$

- Dirac equation:

$$i\vec{\gamma}\cdot\vec{\partial} + m + V_S + V_V\gamma_0 + V_{TS}\tau_3 + V_{TV}\tau_3\gamma_0 + V_C[(1-\tau_3)/2]\gamma_0\psi_k = \gamma_0\epsilon_k\psi_k$$

where,

$$V_S = \alpha_S\rho_S + \beta_S\rho_S^2 + \gamma_S\rho_S^3 + \delta_S\Delta\rho_S \quad (10)$$
$$V_V = \alpha_V\rho_V + \gamma_V\rho_V^3 + \delta_V\Delta\rho_V \quad (11)$$
$$V_{TS} = \alpha_{TS}\rho_{TS} + \delta_{TS}\Delta\rho_{TS} \quad (12)$$
$$V_{TV} = \alpha_{TV}\rho_{TV} + \delta_{TV}\Delta\rho_{TV} \quad (13)$$
$$V_C = eA_0 \quad (14)$$

Relativistic point-coupling model

- Lagrangian density:

$$\mathcal{L} = \mathcal{L}^{\text{free}} + \mathcal{L}^{\text{4f}} + \mathcal{L}^{\text{hot}} + \mathcal{L}^{\text{der}} + \mathcal{L}^{\text{em}}$$

Nikolaus PRC1992; Bürvenich PRC2002

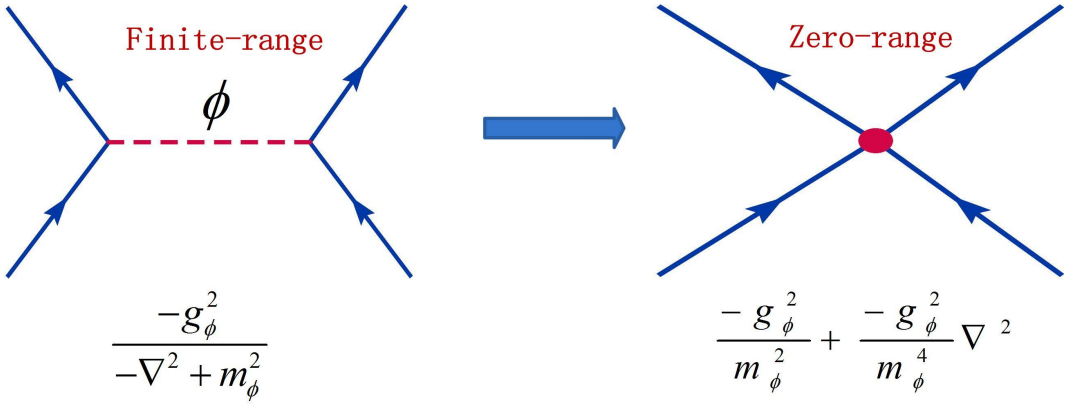

- Mean-field approximation:

$$|\phi\rangle = \prod_{k=1}^{A} a_k^\dagger |0\rangle$$

- Dirac equation:

$$i\vec{\gamma}\cdot\vec{\partial} + m + V_S + V_V\gamma_0 + V_{TS}\tau_3 + V_{TV}\tau_3\gamma_0 + V_C[(1-\tau_3)/2]\gamma_0\psi_k = \gamma_0\epsilon_k\psi_k$$

- Binding energy:

$$\begin{aligned} E_T = & \sum_{k=1}^{A}\epsilon_k - \int d^3\boldsymbol{x}\{\frac{1}{2}\alpha_S\rho_S^2 + \frac{1}{2}\alpha_V\rho_V^2 + \frac{1}{2}\alpha_{TS}\rho_{TS}^2 + \frac{1}{2}\alpha_{TV}\rho_{TV}^2 \\ & + \frac{2}{3}\beta_S\rho_S^3 + \frac{3}{4}\gamma_S\rho_S^4 + \frac{3}{4}\gamma_V\rho_V^4 + \frac{1}{2}\delta_S\rho_S\Delta\rho_S + \frac{1}{2}\delta_V\rho_V\Delta\rho_V \\ & + \frac{1}{2}\delta_{TS}\rho_{TS}\Delta\rho_{TS} + \frac{1}{2}\delta_{TV}\rho_{TV}\Delta\rho_{TV} + \frac{1}{2}j_p^0 V_C\} \end{aligned} \tag{10}$$

Numerical details

- Identify configuration: quantum number transformation

$$|n_x, n_y, n_z, n_s\rangle \rightarrow |nljm_z\rangle \rightarrow |nljm_x\rangle \tag{11}$$

- Fix configuration: parallel transport

$$\langle \phi_j(\Omega + \delta\Omega) | \phi_i(\Omega) \rangle \approx 1 \tag{12}$$

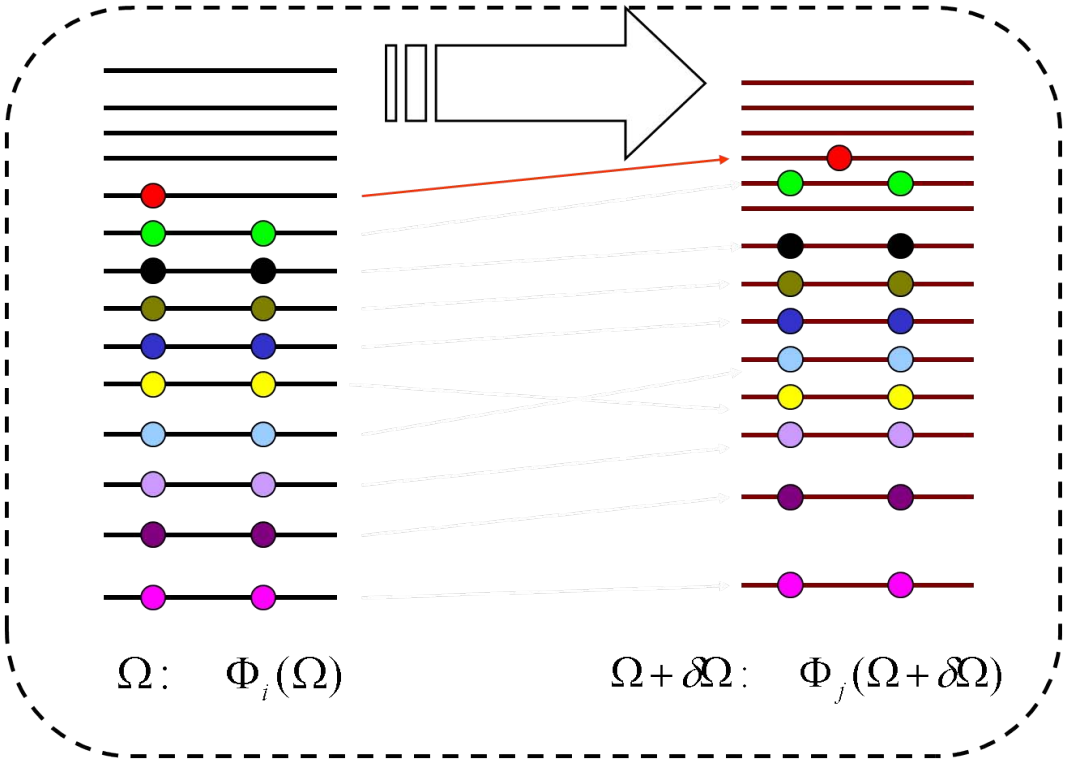

Self-consistency of the tilted axis cranking

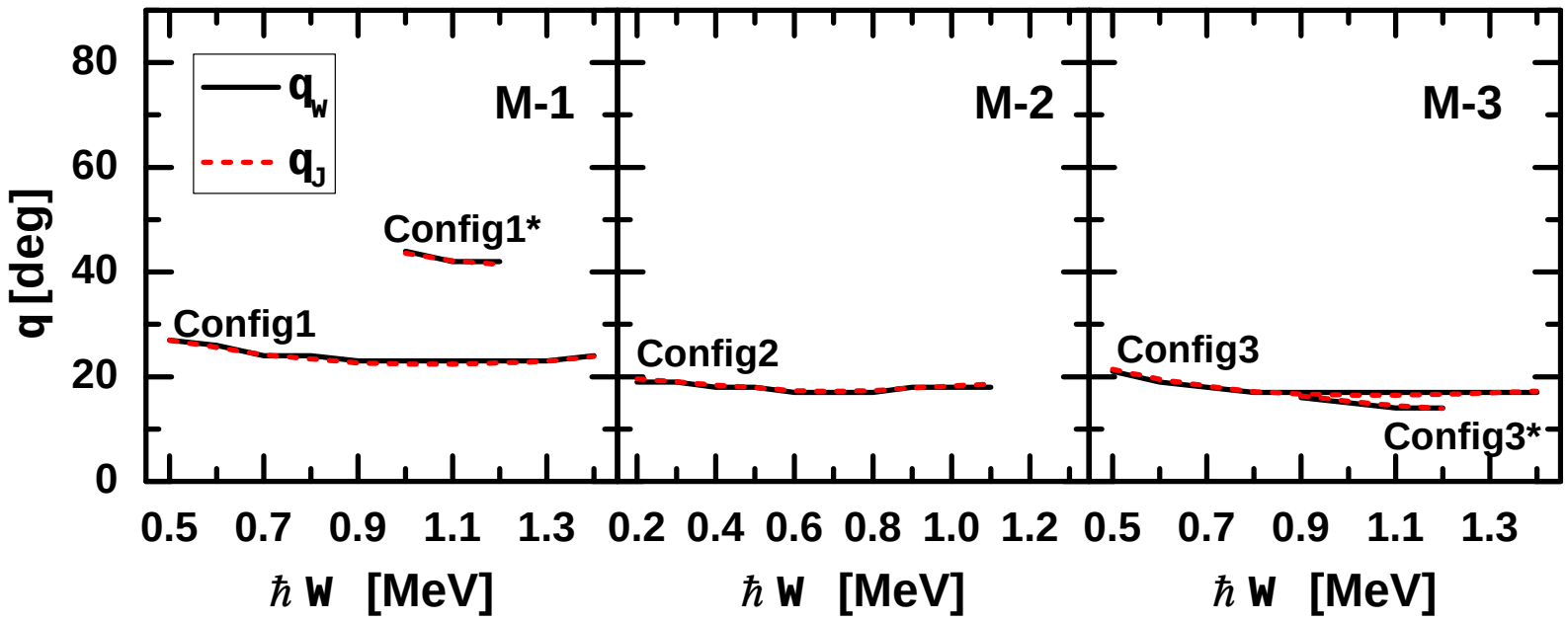

Figure: Tilt angle of the tilted axis θ_Ω and the total angular momentum vector θ_J as functions of the rotational frequency in the tilted axis cranking RMF calculations for band M-1 (left panel), M-2 (middle panel) and M-3 (right panel).

Remarks

a. Self-consistency $\Longrightarrow$ Minimizing total Routhian $\Longrightarrow$ $\boldsymbol{\Omega} \parallel \boldsymbol{J}$.

b. $\theta_\Omega = \theta_J \Longrightarrow$ self-consistency is fully achieved.